Stabilin-1 and Stabilin-2 are specific receptors for the cellular internalization of phosphorothioate-modified antisense oligonucleotides (ASOs) in the liver

Colton M. Miller[1], Aaron J. Donner[2], Emma E. Blank[1], Andrew W. Egger[1], Brianna M. Kellar[1], Michael E. Østergaard[2], Punit P. Seth[2,*] and Edward N. Harris[1,*]

[1]University of Nebraska–Lincoln, Dept. of Biochemistry, 1901 Vine Street Lincoln NE 68588, USA and [2]Ionis Pharmaceuticals, 2855 Gazelle Ct, Carlsbad, CA 92010, USA

ABSTRACT

Phosphorothioate (PS)-modified antisense oligonucleotides (ASOs) have been extensively investigated over the past three decades as pharmacological and therapeutic agents. One second generation ASO, Kynamro™, was recently approved by the FDA for the treatment of homozygous familial hypercholesterolemia and over 35 second generation PS ASOs are at various stages of clinical development. In this report, we show that the Stabilin class of scavenger receptors, which were not previously thought to bind DNA, do bind and internalize PS ASOs. With the use of primary cells from mouse and rat livers and recombinant cell lines each expressing Stabilin-1 and each isoform of Stabilin-2 (315-HARE and 190-HARE), we have determined that PS ASOs bind with high affinity and these receptors are responsible for bulk, clathrin-mediated endocytosis within the cell. Binding is primarily dependent on salt-bridge formation and correct folding of the intact protein receptor. Increased internalization rates also enhanced ASO potency for reducing expression of the non-coding RNA Malat-1, in Stabilin-expressing cell lines. A more thorough understanding of mechanisms by which ASOs are internalized in cells and their intracellular trafficking pathways will aid in the design of next generation antisense agents with improved therapeutic properties.

INTRODUCTION

Second-generation antisense oligonucleotides (Gen 2 ASOs) have made rapid progress in the clinic for the treatment of a variety of disorders (1–4). These drugs are typically modified using the phosphorothioate (PS) linkage which replaces one of the non-bridging oxygen atoms of the phosphodiester linkage with sulfur (5). The PS modification enhances ASO stability from nuclease mediated metabolism and also enhances avidity for plasma, cell-surface and intra-cellular proteins (6).

In animals and in humans, PS ASOs are injected subcutaneously as solutions in saline and do not require special formulations or vehicles to aid their delivery (7). They distribute to all tissues (except across the blood brain barrier) after systemic injection with organs such as the liver, kidneys, spleen, bone-marrow and lymph nodes showing the highest levels of ASO accumulation (8). Within the liver, ASOs distribute to all cell-types but accumulate preferentially in the non-parenchymal endothelial cells lining the liver sinusoids and in Kupffer cells (9,10).

In culture, almost all mammalian cells possess the ability to internalize PS ASOs in a saturable and temperature dependent manner over time (11,12), even in the absence of transfection reagents to help deliver the oligonucleotide across cell membranes. However, cells display different sensitivities toward functional ASO uptake which results in downregulation of the targeted mRNA in the cytoplasm or the nucleus (11,13). Previous work showed that PS ASOs bind avidly to extra-cellular matrix proteins such as fibronectin and laminin (14) and to heparin-binding cofactors such as bFGF in a sequence-independent, but length and PS dependent manner (15). Other studies have implicated scavenger receptors in the uptake of chemically modified ASOs with limited functional consequences (9,16,17). Despite this progress, the identity of specific cell-surface proteins which bind and internalize PS ASOs in a functional manner remains poorly understood (18).

Given the ability of negatively charged PS ASOs to interact with heparin-binding proteins and scavenger receptors, we questioned if the Stabilin receptors could be involved in the uptake of PS ASOs into cells and animals. The Stabilins are class H scavenger receptors which clear negatively

charged and/or sulfated carbohydrate polymer components of the extracellular matrix from circulation (19). They are large type I receptors composed of four Fasciclin-1 domain clusters, four epidermal growth factor (EGF)/EGF-like clusters and one X-Link domain near the single transmembrane region. Although the human Stabilin-1 and Stabilin-2 extracellular portions of the receptors (>96% of the protein) are 55% homologous, the short intracellular domains are very diverse which contributes to differences in their location within the cell, cycling from the plasma membrane and downstream signaling activities.

The receptors share some of the same ligands such as advanced glycation end-products (20), heparin (21,22) and other glycosaminoglycans, forms of low-density lipoprotein (23,24), and GDF-15 (25). In addition, several ligands are unique to each receptor such as lactogen (26) and SPARC (secreted protein acidic and rich in cysteine) (27) for Stabilin-1 and hyaluronan (HA) (28) and some of the chondroitin sulfates for Stabilin-2 (29). Stabilin receptors possess very low to no binding affinity for natural nucleic acids containing phosphodiester bonds (30).

Stabilin-1 is expressed in non-continuous sinusoidal endothelium of liver, spleen, adrenal cortex, lymph node and sinusoidal macrophages (31,32). In fact, recent proteomic databases show that Stabilin-1 is expressed in many tissues throughout the body. Stabilin-2 is expressed in low levels in several human tissues (http://www.gtexportal.org/home/ (33)), but highly expressed in non-continuous sinusoidal endothelium of liver, lymph node, spleen and bone marrow—tissues which represent sites of high accumulation for PS ASOs in animals (8). In the natural tissue, Stabilin-2 is also different from Stabilin-1 in that it is expressed as two isoforms (315- and 190-kDa) resulting from proteolytic cleavage termed 315-HARE and 190-HARE (Hyaluronic Acid Receptor for Endocytosis) (34). In this report, we demonstrate that the Stabilin receptors are capable of binding and internalizing PS ASOs in a functional manner in cells and tissues.

MATERIALS AND METHODS

Oligonucleotide synthesis and delivery

Phosphodiester and PS ASOs were synthesized using standard phosphoramidite chemistry on a DNA synthesizer at Integrated DNA Technologies (Iowa City, IA, USA) or at Ionis Pharmaceuticals (Carlsbad, CA, USA). The morpholino oligo was synthesized by Gene Tools (Philomath, OR, USA). The radio-labeled ASO was synthesized at 3D Imaging (Little Rock, AR, USA) by reacting an amino-modified ASO with ^{125}I-labeled Bolton-Hunter reagent (Perkin-Elmer). Briefly, purified, desalted 5′-amino modified ASO (1 mg, 130 nmol) was dissolved in 0.1 M sodium tetraborate, pH 8.5 (8 μl) and mixed with Bolton-Hunter reagent (2 mCi) dissolved in anhydrous dimethyl sulfoxide (20 μl) for 2 h. Then 2 M NaOH (20 μl) is added and mixed for 1 h. Conjugate is purified using a Sephadex G-25 NAP column following the instructions from the manufacturer. Conjugate purity is determined using a high performance liquid chromatography (HPLC) system equipped with an Agilent SEC-3 column (7.8 × 300 mm) and a β-RAM counter. Total radioactivity after purification is 1.6

mCi giving an 80% radioactive yield. Sequence (5′ to 3′) of the 20-mer is GCTTCAGTCATGACTTCCTT and the complement is AAGGAAGTCATGACTGAAGC. Modification code: d is DNA, r is RNA, e is 2′O-methoxyethyl (MOE) RNA, m is 2′O-Me RNA, f is 2′F RNA, p is phosphoramidate linked morpholino, all oligos are PS modified except underlined letters which are phosphodiester linked (Figure 1A). ASOs were delivered to cells under gymnotic conditions. Likewise, there was no delivery vehicle for the 'free' ASOs when they were injected into the animals.

Cell lines and primary cells

Stabilin and empty vector (EV) cell lines were generated as previously described (29,34). Briefly, the cDNA of interest was inserted into pcDNA5/FRT/V5–6xHIS-TOPO (Invitrogen) and stably transfected in HEK293 Flp-In cells (Invitrogen). Primary liver sinusoidal endothelial cells were harvested from rat using the method described previously (35) which is a modified protocol provided by Seglen (36).

Animals

CD-1 mice or Sprague-Dawley rats (Charles River) were used for all of the animal experiments using IACUC protocols #956 and #607 at the University of Nebraska. *Half-life in blood determination*: mice were anesthesized with 30% isoflurane in PEG200, injected retro-orbitally with 2.0 mg/kg ^{125}I-ASO and immobilized in a 50 ml conical with the bottom punctured to allow the mouse to breathe. Lidocaine anesthetic cream was applied on the tail and the tail was cut about 2 cm from the end to allow bleeding over the course of 40 min. *Tissue distribution*: after the mice were injected as above, they were placed in a metabolic cage for 30 min to allow for collection of urine. The mouse was re-anaesthetized and tissue and organs were collected. *Liver perfusion*: as above after the re-anaesthetation, a 24 (mice) or 18 (rat) gauge catheter was inserted in the portal vein and the liver was flushed of blood with phosphate buffered saline (PBS) at a rate of 6 (mice) or 15 (rat) ml/min for 3 min. The liver was digested *in situ* with modified buffers containing 0.5 mg/ml collagenase IV (Sigma) for 7 (mice) or 20 (rat) min at 6 (mice) or 20 (rat) ml/min. Cells were purified as described previously (35). Stabilin-2 knockout mice (Stab2 KO) were developed at the University of Tokyo and previously described in Hirose *et al.* (51).

Endocytosis and binding assays

Stable cell lines were plated and allowed to grow 2 days prior to the experiment in Dulbecco's modified Eagle's medium (DMEM) + 8% fetal bovine serum (FBS) with 50 μg/ml Hygromycin B. For the primary cells, all assays were performed the same day as the purification and cells were allowed to recover at least 3 hrs prior to the experiment in DMEM + 8% FBS. At the start of the experiment, Assay Medium (DMEM + 0.05% BSA) was prepared with 0.1 μM ^{125}I-ASO without or with ASO competitors (20 μM). The incubation time as indicated was either at 37°C for endocytosis or on ice (1–4°C) for binding. Following incubation, the cells were washed with Hank's Balanced Salt Solution

(HBSS) followed by quantification of isotope in counts per minute (CPM) and cell lysate protein in micrograms (μg) by radiography and Bradford assays, respectively. For experiments requiring receptor specific endocytosis, CPM/μg protein from extra wells containing labeled ASO with a 200-fold excess of the same unlabeled ASO were subtracted from the experimental samples. The data was calculated as the mean $\pm$ SD. Clathrin-dependent endocytosis was evaluated by incubating the cells with 0.4 M sucrose (34), 30 μM Pit-Stop2 (37), 300 μM Dynasore (38) beginning at 30 min prior to the addition of ligand and throughout the experiment (1 h).

Direct (ELISA-like) binding assays

The secreted 190-HARE protein purification and details of the assay are previously described (24). In these assays, 1.0 μg/ml (200 ng/well) s190 protein was used for plating in the plastic polysorp (Nunc, 469 957) wells and incubated overnight at room temperature. All incubations with competitors and salt conditions were performed at 37°C for 1 h followed by 4–5 washes with tris-buffered saline (TBS)-0.1% Tween 20. Wells were washed twice with 1% sodium dodecyl sulphate to harvest bound ^{125}I-ASO, which was then quantified by a gamma counter.

Confocal microscopy

190-HARE, Stab1 and EV cells were incubated with a Cy3-ASO for 1, 3 and 6 h followed by an incubation of 0.5 μM LysoTracker Green or 0.5 μM ERTracker Green for 25 min. Cells were washed with phenol red-free DMEM and imaged using Olympus Fluorview 500, mounted on an Olympus IX81. The images were captured using Fluorview version 5.0 and analyzed with Fiji 2.0 software (39). For this analysis, the fluorescent channels were split, and analyzed using the Coloc2 function. The red fluorescence was set to channel one, with green fluorescence being set to channel two, with the region of interest being set to channel one due to slight background autofluorescence. Colocalization data was determined using Pearson's Correlation coefficient.

Degradation assay

Cells were cultured in 100 mm plates at least 2 days prior to the experiment. Next, cells were incubated for 2 h with Assay Medium containing 0.1 μM ^{125}I-ASO, washed 5$\times$ with HBSS, and then incubated for 6 h with fresh Assay Medium. The medium was harvested, centrifuged to clear away cell debris and then passed over a diethyl-aminoethyl (DEAE) column containing 1 ml of resin. The resin was washed with 0.75 ml 0.4 M NaCl 10 times to collect small fragments and washed with 0.75 ml 2.0 M NaCl three times to collect the larger fragments. The washes containing ASO fragments and resin containing intact ASO were assessed by a gamma counter. As a positive control for degradation, ASO was incubated in 2 M HCl for 1 h at 90°C. To determine if ASOs were degraded in mouse urine, mice were injected intravenously with 2.0 mg/kg ^{125}I-ASO, allowed to circulate for 1 h while the mice were in metabolic cages and all urine was collected from the cage collection vials and from the

bladder of each mouse. The urine was passed through the DEAE column as described above.

Malat-1 expression

Cells were cultured in 96-well plates and then incubated with malat-1 ASO for 24 and 48 h without any transfection agent. Cells were washed once with PBS and total RNA was harvested and gene expression was evaluated by qPCR using malat-1 primers, for 5′-AAAGCAAGGTCTCCCCACAAG-3′, rev 5′-TGAAGGGTCTGTGCTAGATCAAAA-3′, probe 5′-TGCCACATCGCCACCCCGT-3′ and GAPDH primers, for 5′-GAAGGTGAAGGTCGGAGTC-3′, rev 5′-GAAGATGGTGATGGGATTTC-3′, probe 5′-CAAGCTTCCCGTTCTCAGCC-3′.

siRNA delivery

Stab1 and Stab2 cell lines were plated in 24-well plates and allowed to grow to 50% confluency followed by transfection of 5 pmol siRNAs consisting of 2.5 pmol of each of two siRNAs specific for the receptor or scrambled controls using RNAiMAX lipofectamine (Invitrogen). After 48 h, a standard endocytosis assay using 0.1 μM ^{125}I-ASO was performed on the cells. Two siRNAs were designed and purchased from SilencerSelect (Ambion) for each Stabilin receptor and the sequences for Stab1 are 5′-GGAUGAUGAGCUCACGUAUtt-3′ and 5′-CCACGUUUGUCACUCAUGUtt; for Stab2 are 5′-GGAUUAUGAAGGUGACGGAtt-3′ and 5′-GUGAUAUCAUCAGUACUAAtt-3′. Negative/scrambled and positive/GAPDH controls were pre-stocked with catalog numbers 4 390 843 and 4 390 849, respectively.

Immunohistochemistry

Immunohistochemistry for PS ASO in spleen, liver and kidney of animals administered 10 mg/kg ASO and sacrificed 72 h later. Tissues were fixed in 10% neutral buffered formalin, dehydrated in graded ethanol, embedded in paraffin, sectioned and stained using an antibody against the ASO (generated in-house) and counter-stained with hematoxylin. Tissue images were acquired using an Aperio scanner.

Statistics

Unless otherwise stated, all statistics were calculated using Student's t test for pairwise comparisons using SigmaPlot v11.2.

RESULTS

ASO chemistry and design

PS modified Gen 2 ASOs have a central region of DNA flanked on either end with 2′-modified nucleotides such as MOE RNA (Figure 1) (40). The DNA region serves as the substrate for RNase H recognition while the MOE nucleotides enhance RNA-binding affinity and metabolic stability. For our experiments, MOE-DNA ASO (ASO) was
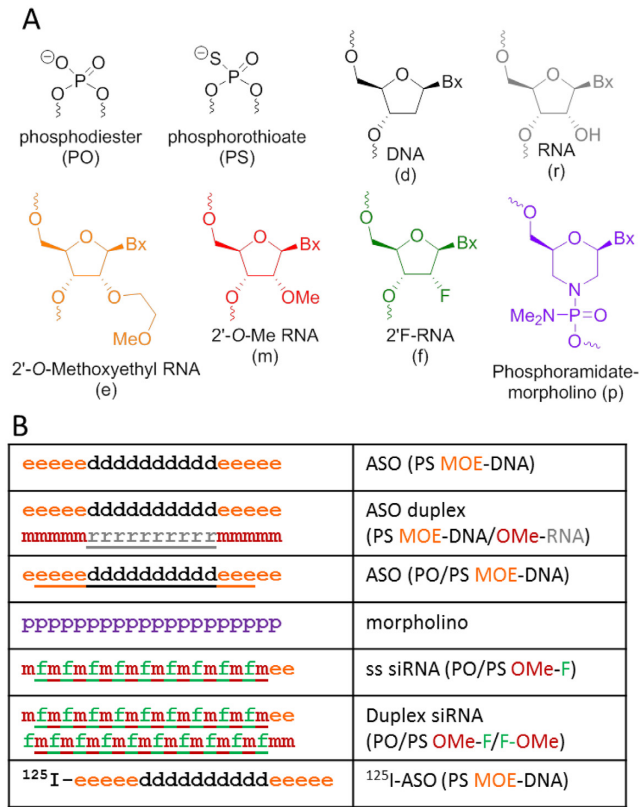
Figure 1. Illustration of antisense oligomers (ASO) and morpholinos. (**A**) Detailed structure of each ASO sugar backbone with elemental or organic modifications on the 2′ carbon of ribose excluding the morpholino (purple). (**B**) Full length structure of each specific ASO compound or morpholino as indicated by the letters in part A. Underlined letters are nucleosides linked with phosphodiester bonds otherwise the nucleosides are linked with phosphorothioate (PS) linkages.

radiolabeled with ^{125}I and used as a standard marker for endocytosis and binding for all subsequent experiments in this report (Figure 1B, bottom).

ASO sequestration in liver

We first injected mice intravenously to determine the half-life of the radiolabeled ASO in blood. Time zero was established 1 min after the initial injection and then samples from the tail-vein were taken every min for up to 40 min (Figure 2A). From these results, we estimated the half-life of ^{125}I-ASO in murine circulation is about 9.5 min. Based on this information and in previous reports (10), we harvested tissues, blood and urine at 30 min post-injection to determine where the ASO accumulates.

The radiolabeled ASO was widespread and could be found in all tissues examined; however, we harvested tissues with important hematological functions and determined that the bulk of the injected ASO accumulates in the liver, followed by kidney (Figure 2B). Liver accumulation occurs as a function of time, whereas, the kidney, which filters the bloodstream and produces urine, becomes saturated with PS oligo very quickly.

The liver is composed of four primary cell types. The hepatocytes comprise over 80% of the liver mass while the liver
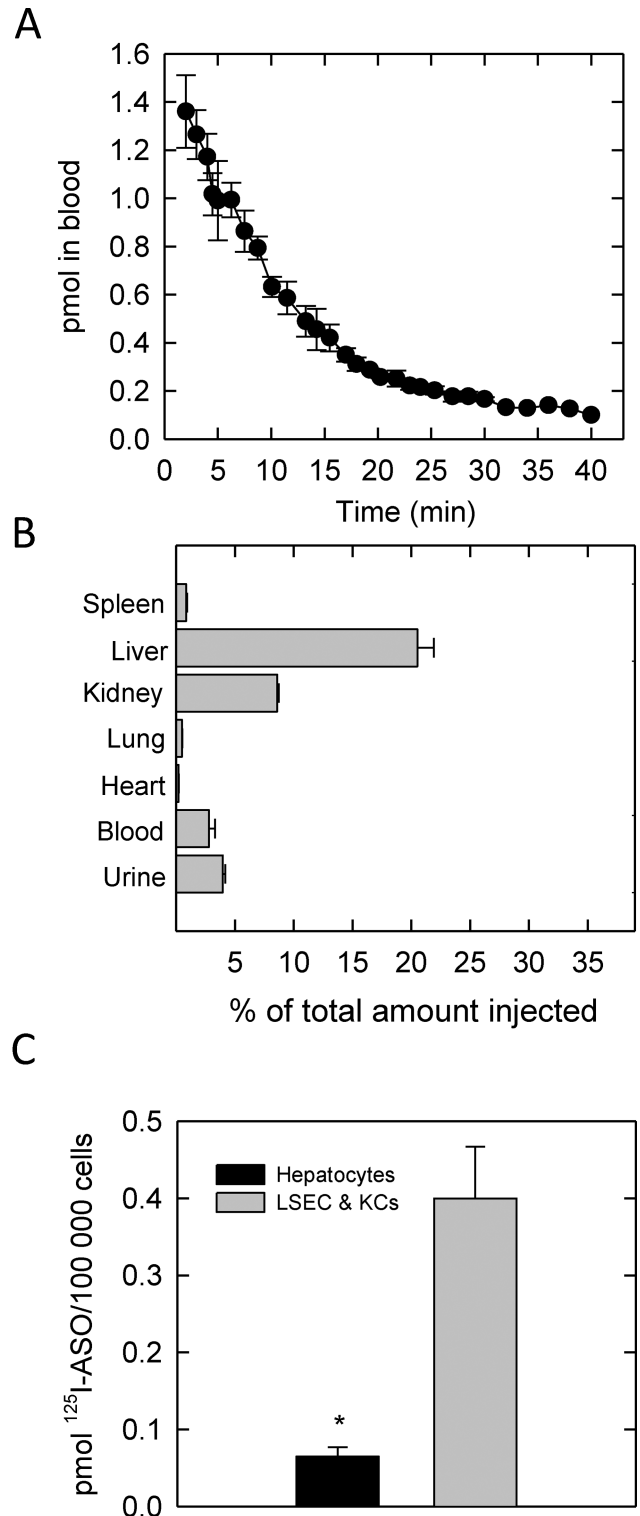

Figure 2. Half-life and tissue distribution of ASO in mice. (**A**) Half-life of 2 mg/kg ASO in blood of mice injected intravenously. A small volume (10–30 μl) of blood was obtained from tail-bleeds about every minute over the course of 40 min and measured for radioactivity and volume. (**B**) Distribution of ASO in hematological tissues including blood and urine after intravenous injection. (**C**) After intravenous ASO injection, the liver was flushed, perfused with collagenase and hepatocytes were purified followed by the enriched pool of LSECs and Kupffer cells. For all experiments, at least three mice were used. Data points are mean ± SEM, (*) $P < 0.05$.

sinusoidal endothelium (LSECs), Kupffer cells (KCs) and hepatic stellate cells (HSCs) account for <10%. To determine which cell type had the highest accumulation of ASO, we perfused the liver of mice 30 min post-injection with collagenase and proceeded to purify hepatocytes and the non-parenchymal fraction which is composed of LSECs and KCs. From our data, the LSECs and KCs together accumulated ~4-fold more ASO than the hepatocytes, suggesting that these cells possess a mechanism to sequester ASO from the blood (Figure 2C).

HEK-293 cells stably expressing Stabilin-1 and -2 receptors internalize PS ASOs by clathrin-mediated endocytosis

The Stabilin receptors are highly expressed in primary LSECs and to a lesser extent in KCs. These receptors were previously cloned and stably expressed in the HEK293 Flp-In cell line system (29) as primary cells quickly lose receptor expression in culture. Relative expression of these protein receptors in recombinant cell lines was determined by western analysis (Figure 3A). Our cell lines stably express Stabilin-1, Stabilin-2/315-HARE (containing the 315 and 190 kDa isoforms), Stabilin-2/190-HARE (containing only the 190-kDa isoform) and the EV line which is stably transfected with the plasmid backbone without any cDNA insertion under hygromycin B selection and acts as a negative control for the Stabilin expressing cell lines.

With these four cell lines, we allowed cells to internalize ^{125}I-ASO under gymnotic conditions over the course of 9 h and found that the 190-HARE cells had the highest internalization rates followed by 315-HARE, Stab1 and EV with the lowest rate (Figure 3B). Specific endocytosis by the Stabilin receptors was also confirmed by siRNA knockdown of each receptor in the Stabilin cell lines (Supplementary Figure S1A–C).

To determine if the stabilin-mediated ASO internalization occurs via clathrin-mediated endocytosis (34), all four cell lines were treated with PitStop2 which interferes with the clathrin terminal domain function (37) and Dynasore which inhibits the GTPase function of dynamin in coated pit formation (41). Treatment with these drugs, and with sucrose induced-hyperosmolarity, did not affect the small amount of ASO internalized by the EV cells (Figure 3C), but all Stabilin cell lines had reductions in 50–85% of uptake (Figure 3D–F).

The EV cells do internalize some ASO and initially had quick uptake rates suggesting that the ASO bound to proteins/receptors on the cell membrane. To test this, we placed cells on ice with ^{125}I-ASO for 1.5 h to inhibit endocytosis, but not binding. All four cell lines bound with approximately the same amount of ASO suggesting that chemical properties of the ASO allow it to bind cell surface proteins, but internalization is largely accomplished by specific receptors (Figure 3G).

Specific binding characteristics of ASO and Stab2/190-HARE

A fifth cell line was created that secretes the smaller Stabilin-2 isoform (s190) in the media for subsequent purification by metal chelate chromatography. The s190 ecto-domain has all the same characteristics as the membrane-bound 190-HARE (24). To verify that the ^{125}I-ASO bound the receptor in measurable quantities, the s190 and bovine serum albumin (BSA) proteins were plated separately on polysorp plastic wells with increasing amounts of labeled ligand. We found that s190 bound increasing concentrations of ^{125}I-ASO with an estimated K_d of 140 nM from this and other experiments (Figure 4A). BSA and other proteins such as DJ-1/PARK7 used as negative controls (Supplementary Figure S2) did not bind with ASO at the concentrations tested.

Next, we investigated the binding characteristics of the ASO and s190. Using increasing concentrations of NaCl for disrupting salt bridges, urea for disrupting hydrogen bonding and guanidinium chloride (GuCl) for protein unfolding, we found that NaCl and GuCl disrupted the interaction between s190 and ASO suggesting that an intact and properly folded s190 protein binds with the ASO via ionic bonding (Figure 4B). This finding is in line with previous reports demonstrating the importance of ionic binding with cell surface proteins (42,43).

Competition with other chemically modified ASOs

To define the structural attributes of chemically modified ASOs for interaction with the Stabilin receptors, competition experiments to block only the internalization of ^{125}I-ASO were performed. A variety of chemical modifications that are commonly used to enhance metabolic stability and other pharmacological properties of therapeutic oligonucleotides were examined (Figure 1). The MOE-DNA configuration facilitates RNase H cleavage of the RNA strand in a RNA/DNA heteroduplex. The charge neutral phosphoramidate morpholino (PMO) chemical class does not support RNase H cleavage but can be used to modulate RNA splicing (44). The single stranded or duplexed alternating 2′-F RNA and 2′-OMe RNA (F-OMe) modification pattern is the leading chemical design for harnessing the RISC mechanism in the clinic (45,46).

PS versus PO and neutral backbone. We examined the ability of single stranded ASOs with PS, PO and neutral backbone (morpholino) and a PS ASO/RNA duplex to block internalization of ^{125}I-ASO into EV, Stab1, 315- and 190-HARE expressing cell lines. Internalization of ^{125}I-ASO could be completely blocked by the PS ASO and the PS ASO/RNA duplex but not the neutral PMO. The PO/PS ASO (PO is represented by underlined letters in the figure legend) was able to partially block uptake of ^{125}I-ASO in all cell lines suggesting that uptake is charge and PS dependent but not affected by single-stranded or the duplex nature of the PS-ASO (Figure 5A–D).

Impact of length on endocytosis. Next, we examined the ability of single stranded ASOs of different lengths but similar chemistry (20- to 10-mers PS MOE-DNA), 20-mer PO MOE-DNA, ss siRNA and duplex siRNA with a different chemical modification patterns (PO OMe-F), to block uptake of ^{125}I-ASO into the Stabilin-2 190-HARE cell line (Figure 6A) and in primary purified LSECs from rat (Figure 6B). We found that the ability of the PS MOE-DNA to
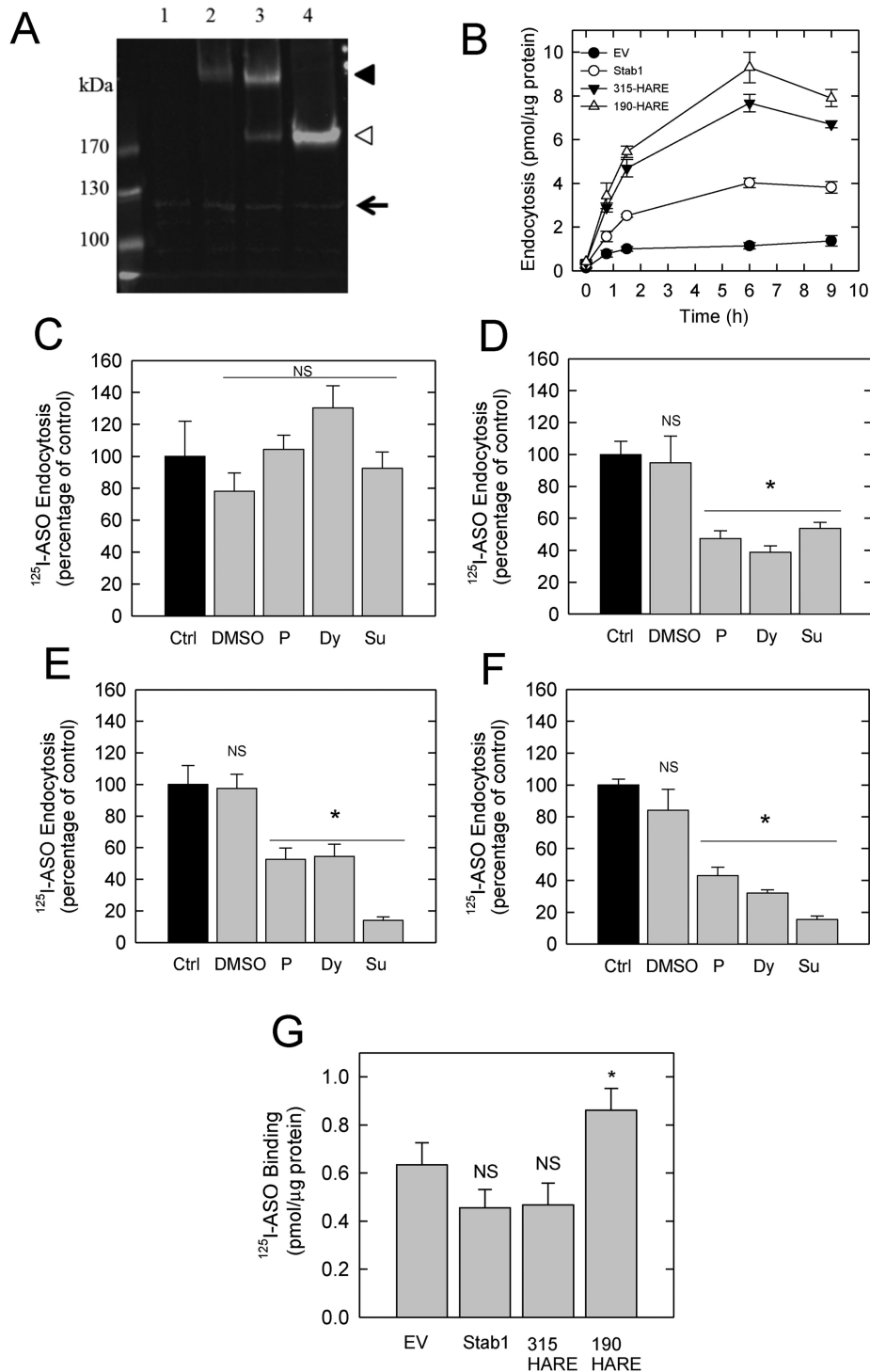
Figure 3. Endocytosis of ASO in Stabilin-expressing stable cell lines. (**A**) Thirty micrograms of whole cell lysate was separated by 5% sodium dodecyl sulphate-polyacrylamide gel electrophoresis, blotted and probed with anti-V5 (against recombinant Stabilin-1, -2) and anti-Vinculin antibodies. Lane 1, empty vector (EV); Lane 2, Stabilin-1; Lane 3, Stabilin-2 (315-HARE); Lane 4, Stabilin-2 (190-HARE). The arrow indicates the Vinculin load control, the black arrowhead indicates the large isoform of Stabilin-2 and Stabilin-1, and the white arrowhead indicates the small isoform of Stabilin-2 (190-HARE). (**B**) All four recombinant cell lines were cultured in 24-well plates, then exposed to 0.1 μM ^{125}I-ASO for 9 h. At each time point, cells were washed 3× with 1.0 ml HBSS, lysed in 0.3 ml 0.3 N NaOH and cell lysates were measured for radioactivity and protein content. The data shown represent total binding of each sample in triplicate as mean ± SD. (**C–F**) Endocytosis of 0.1 μM ^{125}I-ASO in EV (C), Stabilin-1 (D), 315-HARE (E) and 190-HARE (F) cell lines at one time point (90 min) as either untreated control (black bars) or with drugs/conditions (gray bars) that inhibit clathrin-mediated endocytosis. Dimethyl sulfoxide solvent control, P—30.0 μM PitStop2, Dy—300.0 μM Dynasore, Su-0.4 M sucrose. Cells were processed as described in 'Materials and Methods' section and the data represent the mean ± SD, $n = 4$. The asterisk (*) is $P < 0.001$. (**G**) All four cell lines were cultured in 24-well plates, then placed on ice to inhibit endocytosis. Ice-cold medium containing 0.1 μM ^{125}I-ASO was incubated with the cells for 1 h, followed by washing in cold HBSS 3×. Radioactivity and protein were measured and the data is expressed as the mean ± SD, $n = 3$. The asterisk (*) is $P = 0.038$.
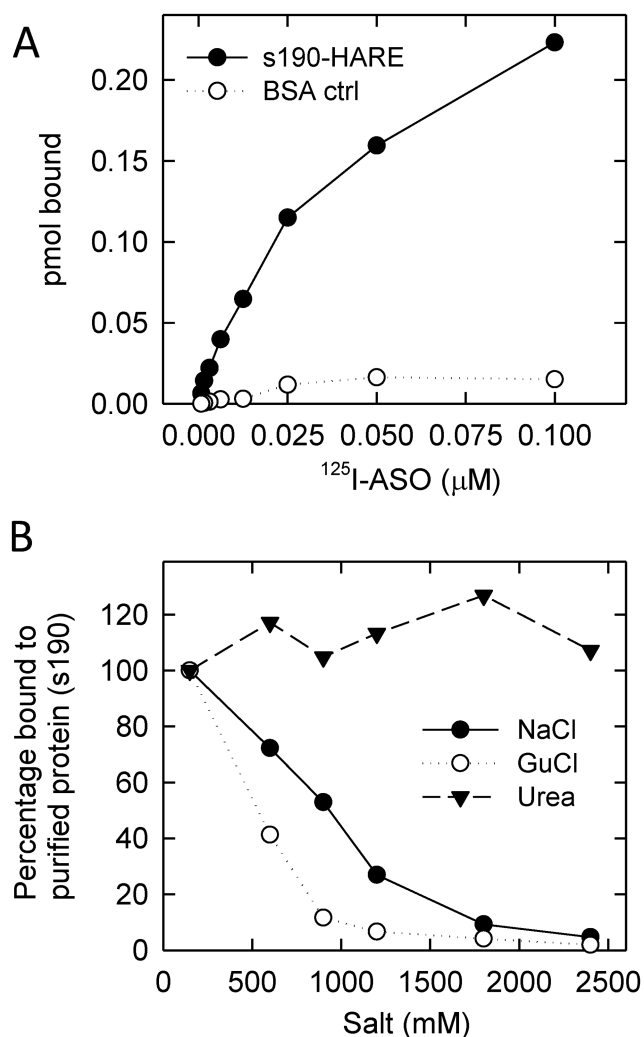
Figure 4. Direct binding assays reveal ASO binding specifically to Stabilin-2/190-HARE. (**A**) A total of 200 ng of s190 (secreted form of the 190-HARE receptor) was placed in polysorp wells with increasing concentrations of ^{125}I-ASO, washed with TBS-tween and the amount bound was measured by a gamma counter. (**B**) Direct binding assay as indicated above with 0.05 μM ^{125}I-ASO incubated in the presence of increasing salt concentrations (150–2500 mM) at 37°C for 1 h. The wells were processed as described in the 'Materials and Methods' section and radioactivity was measured by a gamma counter. All data points are in duplicate.

block uptake was dependent on length as well as PS and charge content. The 20-mer PO MOE-DNA does not compete as efficiently as the 20-mer PS MOE-DNA but better than the PO/PS single stranded and duplex F-OMe siRNA suggesting that PS DNA and charge are the primary pharmacophores for Stabilin-2 recognition. These results are also consistent with previous experiments where similar designs of competitor oligonucleotides were able to interfere with functional uptake of ASOs in cultured cells (11—see Figure 3).

Direct binding. Using the ELISA-like or direct-binding assay, we measured remaining bound ^{125}I-ASO in the presence of increasing amounts of PO MOE-DNA, PS MOE-DNA and ss siRNA (OMe-F). As seen in the competition assays,

PS MOE-DNA varying in length from 20- to 16-mer were all highly competitive in contrast to PS MOE-DNA 14- and 12-mers and 20-mer PO MOE-DNA which were moderately competitive, and, finally, the PO ss OMe-F which did not compete (Figure 6C).

ASO delivery to lysosomes and subsequent degradation

Once ASO is internalized, does the cargo get delivered to lysosomes? We incubated 190-HARE (positive control) and EV (negative control) cells with Cy3-ASO (red) for 1, 3 and 6 hr followed by staining the cells with LysoTracker (green) to visualize lysosome colocalized with Cy3-ASO (Figure 7A). Consistent with our endocytosis assays, the 190-HARE cells internalized much more of the ASO than the EV cells. We also observed more colocalization of the ASO with lysosomes (47) in the 190-HARE cells which increased over the time course as observed by confocal microscopy (Figure 7A) and quantified by Fiji (2.0) software (Figure 7B).

Since Stabilin-1 traffics to the *trans*-Golgi network (TGN) as well as to lysosomes, (48) we asked if the ASO is involved with retrograde transport to the ER. We incubated Stabilin-1 cells under the same conditions with both LysoTracker and ERTracker. By confocal microscopy, it was determined that the ASO is primarily targeted to lysosomes and not to the ER (Supplementary Figure S3A and B).

To determine if the PS ASO is degraded in lysosomes, we cultured both Stabilin-2 cell types and EV cells in 100 mm dishes and incubated them with ^{125}I-ASO for 2 h, washed, and then chased with fresh medium for 6 h. Any ASO in the fresh medium would be secreted from the cells after it has gone through the endo-lysosomal compartments. To separate degraded from intact ASO, the fresh medium was poured over a DEAE anion exchange column which retains the intact ASO and allows the fragments of degraded ASO to be eluted by a weak salt solution.

Intact and degraded PS ASO were characterized by their by migration in 2% agarose gel electrophoresis (Supplementary Figure S4A), profile with ESI-MS (Supplementary Figure S4B) and by chromatographic trace profiles on DEAE columns (Supplementary Figure S5A). The amount of degraded ASO was much higher in the Stab2 cell lines than in EV (Figure 8A) which was also noticed in the elution profile from the DEAE column (Supplementary Figure S5 B). We also repeated these experiments with the Stab1 and EV cell lines and found that the elution profiles were very similar, though the ratio of degraded to intact ASO was higher in the Stab1 cells compared to control (Supplementary Figure S5C and D).

We used the same method to determine if the ASO is intact in the urine of our injected mice. Uninjected ^{125}I-ASO and urine containing ^{125}I-ASO was collected from mice 1 hr post-intravenous injection and run through the DEAE columns. The uninjected ASO is more than 95% intact in contrast to the nearly 70% of ASO in urine that is degraded (Figure 8B). The total amount of ASO in urine is still a small fraction (<10%) of the total injected, but indicates that significant degradation occurs as it is excreted from the animal.
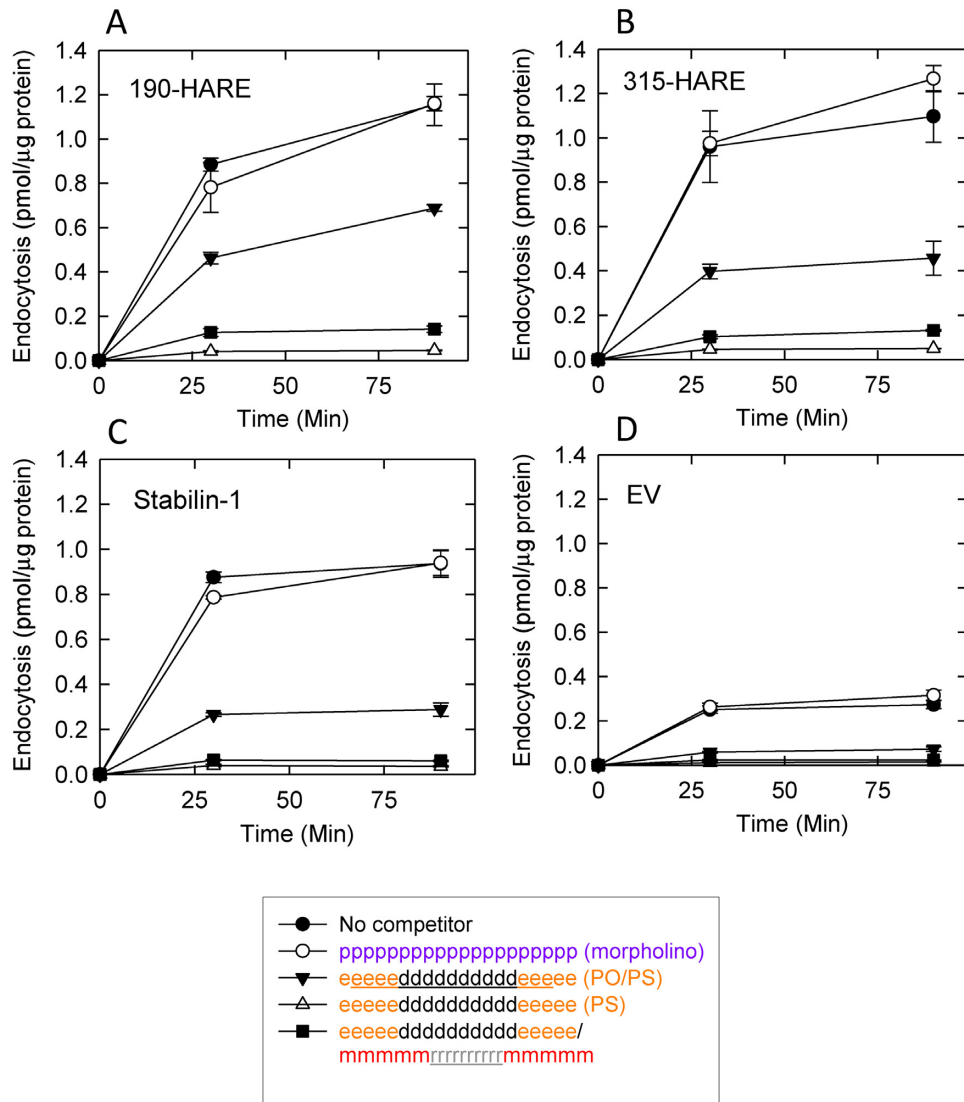
Figure 5. Endocytosis of ^{125}I-ASO with non-labeled competitors in Stabilin cell lines. (**A**) 190-HARE, (**B**) 315-HARE, (**C**) Stabilin-1 and (**D**) EV cells were incubated with 0.1 μM ^{125}I-ASO and 20 μM competitor for up to 90 min at 37°C. At each time point, cells were washed 3× with cold HBSS and solubilized cell lysates were quantified for radioactivity and protein. The data represent the mean ± SD, $n = 4$.

Gene inhibition by ASO in the presence of the Stabilin receptors

Cells in culture were exposed to a PS ASO which targeted *malat*-1 RNA for degradation under gymnotic conditions. *Malat*-1 is a long non-coding RNA (lncRNA) which is highly conserved among all mammals and is associated with metastasis associated genes (49,50). We assessed the expression of *malat*-1 in the four cell lines to determine if endocytosis rates affect specific amounts of malat-1 RNA degradation. Our results show that at both 24 h (Figure 9A) and 48 h (Figure 9B) post-treatments, RNA levels of *malat*-1 are reduced in the Stabilin treated cells compared to EV, suggesting that increased internalization of this ASO enhances antisense activity. Due to comparable expression levels, we compared Stab1 and 315-HARE cells treated with scrambled and Stab-specific siRNAs and determined that a decrease in Stabilin expression resulted in greater malat-1 expression (a decrease in ASO-mediated RNA degradation; Supplementary Figure S6).

ASO accumulation is attenuated in Stabilin-2 KO mice

In our biochemical and cell culture experiments, both Stabilin-1 and Stabilin-2 receptors bound and internalized the ^{125}I-labeled PS ASO, although the Stab2 receptor demonstrated higher endocytic activity than Stab1. As a final confirmation that Stabilin-2 is a primary receptor for ASO uptake in animals, we examined the internalization of PS ASOs in a Stabilin-2 knockout mouse (51) following systemic injection. ASO accumulation in the liver and spleen (high Stabilin-2 expression), and the kidney which does not express Stab2, was examined by immunohistochemistry PS ASO staining in the liver, spleen, and kidney is apparent in the C57BL/6 control parental background in contrast to diminished ASO staining in liver and spleen tissues of
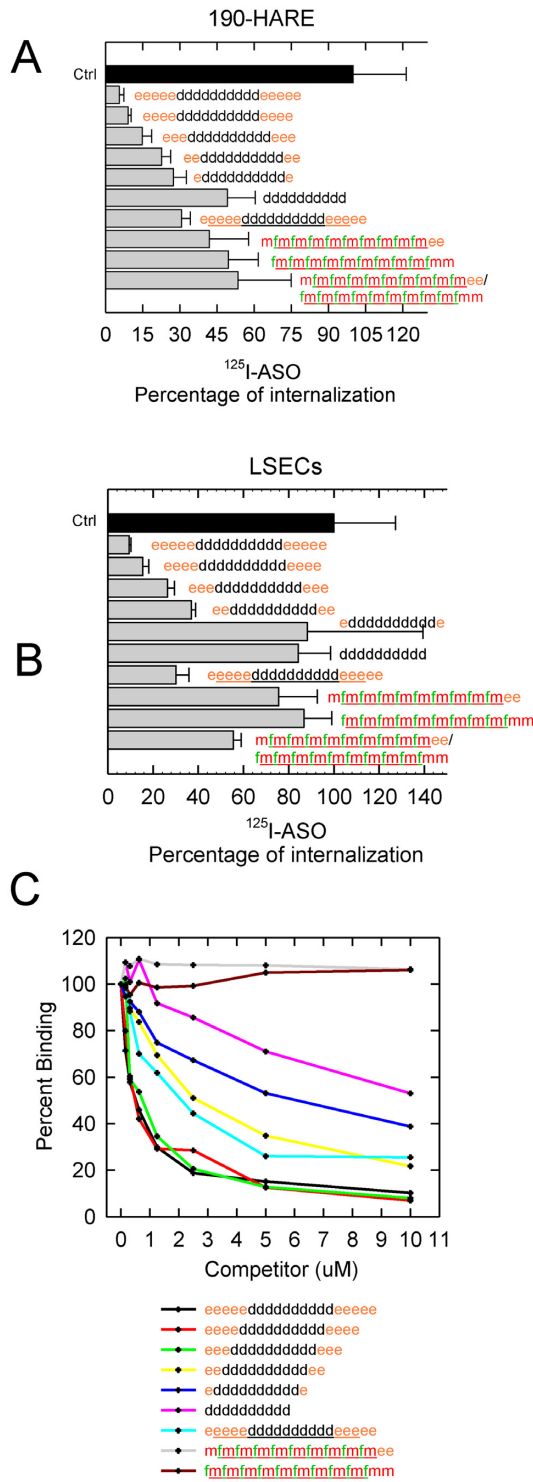
Figure 6. Endocytosis of ^{125}I-ASO in the presence of non-labeled competitors in 190-HARE and primary LSECs. (**A**) 190-HARE and (**B**) primary LSECs from rat were incubated with 0.1 μM ^{125}I-ASO in the presence of unlabeled ASO for 90 min. Cells were processed as described in 'Materials and Methods' section and the data are expressed as the mean ± SD, *n* = 3, as a percentage of the control containing no competitor. (**C**) Inhibition of direct binding of ^{125}I-ASO to s190-HARE by unlabeled ASO competitors. A total of 200 ng of s190-HARE protein was plated in each well along with increasing amounts of indicated competitor (0.156–10 μM) and processed as described in 'Material and Methods' section. All data points are in duplicate.
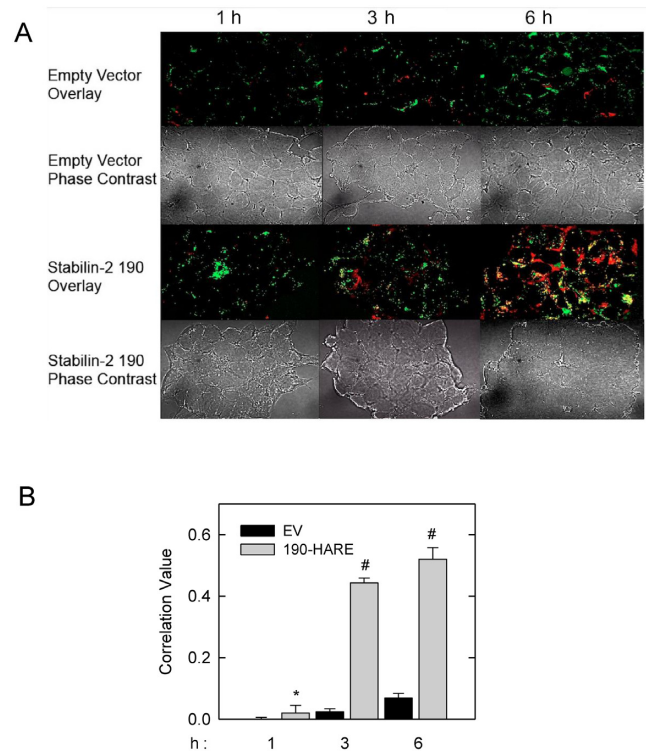

Figure 7. Internalized ASOs traffic to the lysosome. (**A**) 190-HARE and EV cells were incubated with Cy3-ASO (red) for 1, 3 and 6 h, followed by a 25 min incubation with LysoTracker (green). Overlay of the images taken by confocal microscopy generated areas of yellow indicating colocalization of ASOs in lysosomes. (**B**) Quantitative analysis of red versus green versus yellow was based on channel splitting and overlay using Fiji Coloc-2 software. Data is expressed as the mean of at least six images at each time point for each cell line and statistically analyzed using Pearson's correlation coefficient. The asterisk (*) is *P* < 0.001.

the Stab2 KO mouse. These results further confirmed that Stab2 is one of the primary endocytic receptors for PS ASOs in these tissues (Figure 10).

DISCUSSION

Antisense oligonucleotide therapy is an emerging area of clinical-based treatment of chronic disease through gene regulation. PS ASOs are polyanions and bind to a host of extra-cellular matrix proteins such as heparin binding proteins, VEGF, fibronectin and several others through ionic interactions, and with significantly higher affinity than phosphodiester oligonucleotides (52). In our recombinant cell model, PS ASOs bound to the EV cells as well as to the recombinant Stabilin cell lines with near equal affinity. The 190-HARE cell line had just a slightly, but barely, significantly higher binding capacity that may be attributed to the higher numbers of 190-HARE on the cell surface.

Both Stabilin-1 and Stabilin-2 receptors are constitutively active in that internalization occurs with or without cargo (53–55). Thus, cells expressing these receptors internalize ligand more efficiently as compared to the EV line. In all the endocytosis experiments of which only a small subset are shown in this report, the 190-HARE always had the highest endocytosis rates, followed by the large isoform, 315-HARE
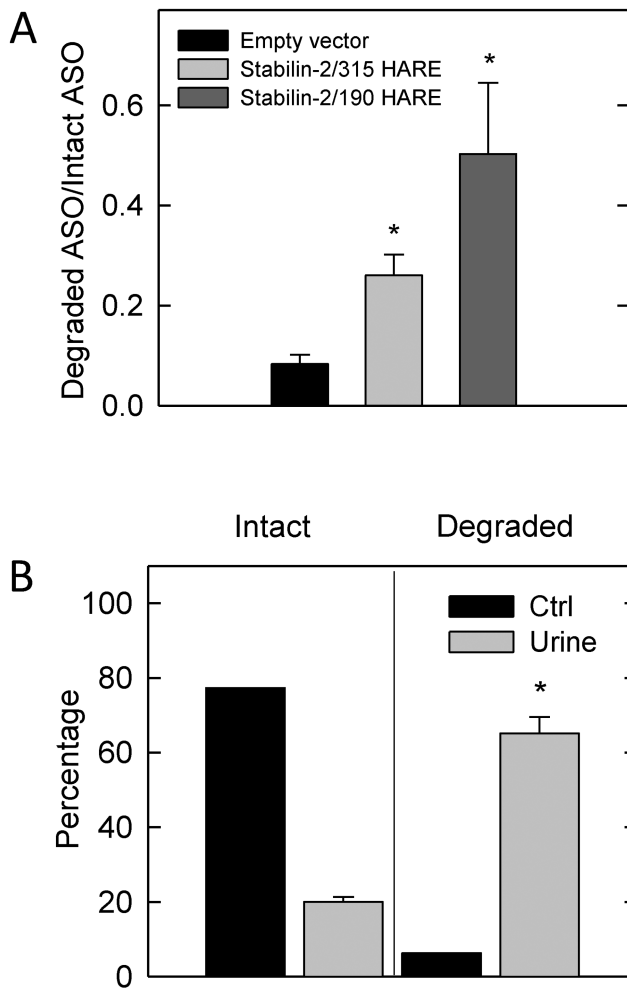
Figure 8. ASOs are degraded in lysosomes and found in the urine of mice. (**A**) 315-HARE, 190-HARE and EV cells were incubated with 0.1 μM ^{125}I-ASO for 2 h, washed and incubated in fresh Assay Medium for 6 h. Intact ^{125}I-ASO in fresh medium was separated from degraded ^{125}I-ASO by DEAE chromatography and the data are expressed as a ratio of degraded to intact ASO, $n = 3$, mean ± SEM. The asterisk (*) is $P < 0.05$. (**B**) 0.01 μM ^{125}I-ASO (black bars, uninjected) and mouse urine (gray bars) was processed the same as in part A. The data represents the mean ± SEM, $n = 5$. The asterisk (*) is $P < 0.001$.

Figure 9. *Malat*-1 gene expression knockdown is more efficient in Stabilin-expressing cells than in the EV cells. Cells cultured in 96-well plates were exposed to *malat*-1 ASO (0.001–100 μM) for (**A**) 24 or (**B**) 48 h in all four cell lines without any transfection agent. At the indicated times, cells were assayed for *malat*-1 RNA by qPCR. Each data point represents the mean ± SEM, $n = 3$.

and then Stabilin-1. Stabilin-1 has a relatively low surface expression level and is localized in both, the endosomal and trans-Golgi network pathways (48,56), which may explain a lower rate of endocytosis.

Binding of the radiolabeled PS ASO to the secreted form of the smaller 190-HARE isoform occurs through ionic charges that is likely the result of interactions of the anionic sulfur atom of the PS linkage with the receptor. Unsurprisingly, both Stabilins interact with sulfated polymers (22) and the mechanism for binding with ASOs and heparins appear to be similar. We performed competition experiments with both HA and heparin (unfractionated) to determine the binding site for the ASOs with the Stabilin-2 receptors. HA binds to the Link domain and when modeled with another HA-binding protein (TSG-6) in serum, the tyrosine residues are necessary for this interaction according to an
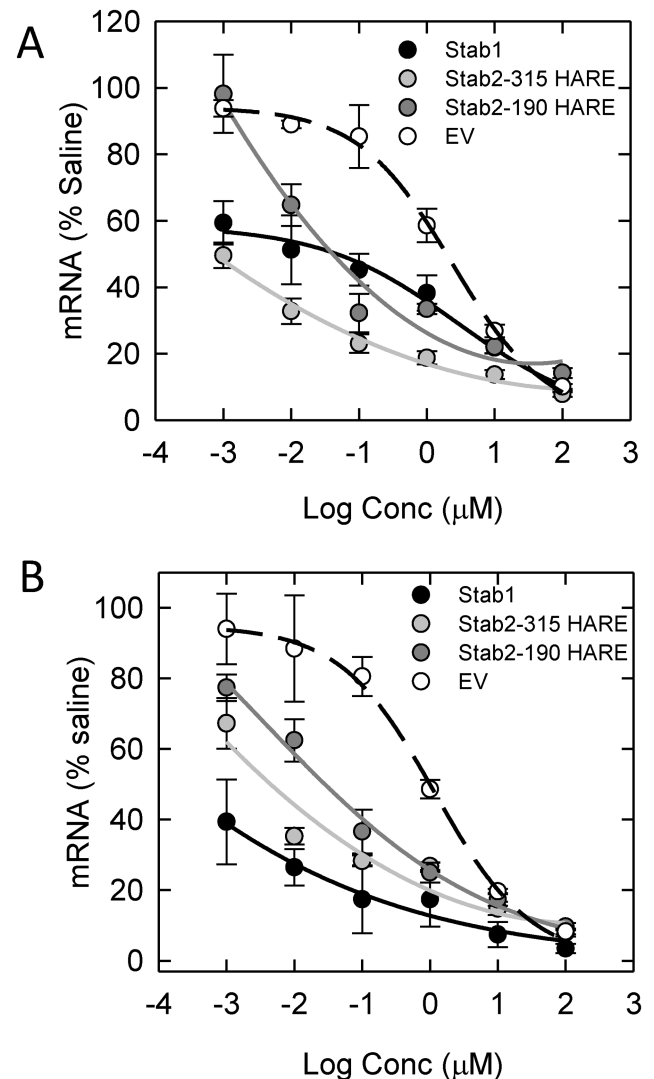
in silico model (57). In the recombinant 315-HARE cells, there was no competition with HA, but the PS ASO was partly competed by heparin suggesting some overlap in the binding site between the negatively charged polymers (Supplementary Figure S7). The heparin binding site(s) are likely within the third and/or fourth EGF clusters found in both Stab2 isoforms, though the details of these sites currently remains unknown on these receptors and we are actively investigating this issue (24).

Stabilin-2-mediated internalization of PS ASOs into transformed or primary cells could be competed using both single and double stranded PS ASOs, but not with neutral linkage morpholinos. Interestingly, chemical designs (PO/PS 2′-F/2′-OMe RNA) commonly used to stabilize single and double stranded siRNA, were less effective at blocking Stabilin-2 mediated binding or internalization of
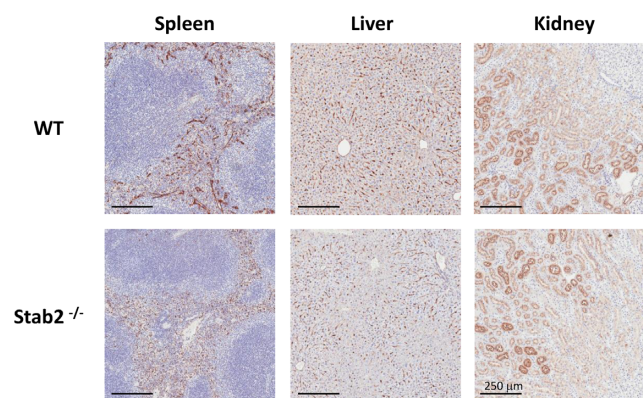
Figure 10. Immunohistochemistry for ASO in spleen, liver and kidney of animals administered 10 mg/kg ASO and sacrificed 72 h later. Tissues were fixed and stained using an antibody against the ASO (generated in-house) and counter-stained with hematoxylin. Tissue images were acquired using an Aperio scanner. Bar, 250 μm.

PS gapmer ASOs, suggesting that PS DNA is an important pharmacophore for stabilin binding. RNA or RNA-like modifications with 2′-electron withdrawing groups exist in the C3'-endo sugar pucker as compared to DNA-like modifications which exist in the C2'-endo sugar conformation (58). Gapmer ASOs are chimeric with regions of both DNA and RNA-like nucleoside modifications. It is conceivable that these conformational changes can modulate interactions of Stabilin-2 with chemically modified oligonucleotides.

Since both Stabilin receptors are targeting their ligands to the endolysomal pathway, how do the ASOs interact with their targets in the cytoplasm or even the nucleus? As seen with the 190-HARE cells, a vast majority of the fluorescent ASO colocalizes with lysosomes (Figure 7A). It is thought that a small percentage of ASO may escape the endosomes, transit through the cytoplasm and may end up in the nucleus by mechanisms that are not fully understood at this time. Indeed, other researchers in the siRNA field have hypothesized the same mechanism is responsible for delivery of specific siRNAs to the cell cytoplasm that were initially internalized by clathrin-mediated endocytosis. Using immunogold techniques, they estimated that between 1–2% of total internalized siRNAs in the cell are trafficked to the site of their bioactivity in the cytoplasm (59).

In our fluorescent imaging, it was not possible to see any fluorescence in the nucleus because of high background resulting from ASO accumulation in endo-lysosomal compartments, but the ASO against *malat*-1 showed enhanced potency in the Stabilin expressing cell-lines as compared to the EV control (Figure 9A and B). These data suggest that a small percentage of ASOs which escape the endolysosomal compartments are sufficient for *malat*-1 knockdown and the process is more efficient in the Stabilin expressing cells than in the EV cells over both time points at most concentrations.

This correlation may well be attributed to an endosomal escape mechanism noting that once the ASO gets internalized via an endosome it has a better chance of membrane penetrance due to the low lipid density and remodeling of endosomal membranes than just binding to the plasma membrane on the cell surface (60,61). Even though the Stabilin-1 cells showed lower endocytosis efficiency, the *malat*-1 knockdown was comparable or better than the high endocytic efficiency of the Stabilin-2 cells. We can only speculate at this time that the differential trafficking pathways of Stabilin-1 in both the endolysosomal and TGN pathways may allow for a higher rate of endosomal escape at most concentrations of ASO incubated with the cells.

In summary, we show that the Stabilin class of receptors can bind and internalize PS ASOs into cells and tissues. The amount of internalized PS ASO increases in cells expressing the Stabilin receptors in contrast to cells that do not express the Stabilin receptors or have been treated with siRNAs against the Stabilin receptors. In the Stabilin-2 KO mouse, liver and spleen tissue lacking Stabilin-2 expression show significantly attenuated PS ASO uptake. It should be noted that while expression of Stabilin proteins coincides with tissues which show high accumulation of PS ASOs in animals, these drugs also accumulate in cells and tissues which do not express Stabilins. The liver and spleen tissues in the Stabilin-2 KO mouse still accumulated a small amount of ASO suggesting existence of additional pathways for ASO internalization. Further studies to better understand the interactions of chemically modified ASOs with cell-surface proteins and their subsequent intracellular trafficking pathways will aid in the design of future antisense agents with improved therapeutic properties.

SUPPLEMENTARY DATA

Supplementary Data are available at NAR Online.

REFERENCES

1. Bennett,C.F. and Swayze,E.E. (2010) RNA targeting therapeutics: molecular mechanisms of antisense oligonucleotides as a therapeutic platform. *Annu. Rev. Pharmacol. Toxicol.*, **50**, 259–293.
2. Büller,H.R., Bethune,C., Bhanot,S., Gailani,D., Monia,B.P., Raskob,G.E., Segers,A., Verhamme,P. and Weitz,J.I. (2015) Factor XI antisense oligonucleotide for prevention of venous thrombosis. *N. Engl. J. Med.*, **372**, 232–240.
3. Gaudet,D., Alexander,V.J., Baker,B.F., Brisson,D., Tremblay,K., Singleton,W., Geary,R.S., Hughes,S.G., Viney,N.J., Graham,M.J. *et al.* (2015) Antisense inhibition of apolipoprotein C-III in patients with Hypertriglyceridemia. *N. Engl. J. Med.*, **373**, 438–447.

4. Tsimikas,S., Viney,N.J., Hughes,S.G., Singleton,W., Graham,M.J., Baker,B.F., Burkey,J.L., Yang,Q., Marcovina,S.M., Geary,R.S. *et al.* (2015) Antisense therapy targeting apolipoprotein(a): a randomised, double-blind, placebo-controlled phase 1 study. *Lancet*, **386**, 1472–1483.

5. Eckstein,F. (2014) Phosphorothioates, essential components of therapeutic oligonucleotides. *Nucleic Acid Ther.*, **24**, 374–387.

6. Liang,X.-h., Sun,H., Shen,W. and Crooke,S.T. (2015) Identification and characterization of intracellular proteins that bind oligonucleotides with phosphorothioate linkages. *Nucleic Acids Res.*, **43**, 2927–2945.

7. Yu,R.Z., Grundy,J.S. and Geary,R.S. (2013) Clinical pharmacokinetics of second generation antisense oligonucleotides. *Expert Opin. Drug. Metab. Toxicol.*, **9**, 169–182.

8. Yu,R.Z., Kim,T.-W., Hong,A., Watanabe,T.A., Gaus,H.J. and Geary,R.S. (2007) Cross-species pharmacokinetic comparison from mouse to man of a second-generation antisense oligonucleotide, ISIS 301012, targeting human apolipoprotein B-100. *Drug Metab. Dispos.*, **35**, 460–468.

9. Bijsterbosch,M.K., Manoharan,M., Rump,E.T., De Vrueh,R.L., van Veghel,R., Tivel,K.L., Biessen,E.A., Bennett,C.F., Cook,P.D. and van Berkel,T.J. (1997) In vivo fate of phosphorothioate antisense oligodeoxynucleotides: predominant uptake by scavenger receptors on endothelial liver cells. *Nucleic Acids Res.*, **25**, 3290–3296.

10. Graham,M.J., Crooke,S.T., Lemonidis,K.M., Gaus,H.J., Templin,M.V. and Crooke,R.M. (2001) Hepatic distribution of a phosphorothioate oligodeoxynucleotide within rodents following intravenous administration. *Biochem. Pharmacol.*, **62**, 297–306.

11. Koller,E., Vincent,T.M., Chappell,A., De,S., Manoharan,M. and Bennett,C.F. (2011) Mechanisms of single-stranded phosphorothioate modified antisense oligonucleotide accumulation in hepatocytes. *Nucleic Acids Res.*, **39**, 4795–4807.

12. Zhao,Q., Matson,S., Herrera,C.J., Fisher,E., Yu,H. and Krieg,A.M. (1993) Comparison of cellular binding and uptake of antisense phosphodiester, phosphorothioate, and mixed phosphorothioate and methylphosphonate oligonucleotides. *Antisense Res. Dev.*, **3**, 53–66.

13. Stein,C.A., Hansen,J.B., Lai,J., Wu,S., Voskresenskiy,A., Hog,A., Worm,J., Hedtjarn,M., Souleimanian,N., Miller,P. *et al.* (2010) Efficient gene silencing by delivery of locked nucleic acid antisense oligonucleotides, unassisted by transfection reagents. *Nucleic Acids Res.*, **38**, e3.

14. Guvakova,M.A., Yakubov,L.A., Vlodavsky,I., Tonkinson,J.L. and Stein,C.A. (1995) Phosphorothioate oligodeoxynucleotides bind to basic fibroblast growth factor, inhibit its binding to cell surface receptors, and remove it from low affinity binding sites on extracellular matrix. *J. Biol. Chem.*, **270**, 2620–2627.

15. Benimetskaya,L., Tonkinson,J.L., Koziolkiewicz,M., Karwowski,B., Guga,P., Zeltser,R., Stec,W. and Stein,C.A. (1995) Binding of phosphorothioate oligodeoxynucleotides to basic fibroblast growth factor, recombinant soluble CD4, laminin and fibronectin is P-chirality independent. *Nucleic Acids Res.*, **23**, 4239–4245.

16. Butler,M., Crooke,R.M., Graham,M.J., Lemonidis,K.M., Lougheed,M., Murray,S.F., Witchell,D., Steinbrecher,U. and Bennett,C.F. (2000) Phosphorothioate oligodeoxynucleotides distribute similarly in class A scavenger receptor knockout and wild-type mice. *J. Pharmacol. Exp. Ther.*, **292**, 489–496.

17. Ezzat,K., Aoki,Y., Koo,T., McClorey,G., Benner,L., Coenen-Stass,A., O'Donovan,L., Lehto,T., Garcia-Guerra,A., Nordin,J. *et al.* (2015) Self-assembly into nanoparticles is essential for receptor mediated uptake of therapeutic antisense oligonucleotides. *Nano Lett.*, **15**, 4364–4373.

18. Juliano,R.L., Ming,X., Carver,K. and Laing,B. (2014) Cellular uptake and intracellular trafficking of oligonucleotides: implications for oligonucleotide pharmacology. *Nucleic Acid Ther.*, **24**, 101–113.

19. Murphy,J.E., Tedbury,P.R., Homer-Vanniasinkam,S., Walker,J.H. and Ponnambalam,S. (2005) Biochemistry and cell biology of mammalian scavenger receptors. *Atherosclerosis*, **182**, 1–15.

20. Tamura,Y., Adachi,H., Osuga,J., Ohashi,K., Yahagi,N., Sekiya,M., Okazaki,H., Tomita,S., Iizuka,Y., Shimano,H. *et al.* (2003) FEEL-1 and FEEL-2 are endocytic receptors for advanced glycation end products. *J. Biol. Chem.*, **278**, 12613–12617.

21. Harris,E.N., Weigel,J.A. and Weigel,P.H. (2008) The human hyaluronan receptor for endocytosis (HARE/Stabilin-2) is a systemic clearance receptor for heparin. *J. Biol. Chem.*, **283**, 17341–17350.

22. Pempe,E.H., Xu,Y., Gopalakrishnan,S., Liu,J. and Harris,E.N. (2012) Probing structural selectivity of synthetic heparin binding to stabilin protein receptors. *J. Biol. Chem.*, **287**, 20774–20783.

23. Li,R., Oteiza,A., Sorensen,K.K., McCourt,P., Olsen,R., Smedsrod,B. and Svistounov,D. (2011) Role of liver sinusoidal endothelial cells and stabilins in elimination of oxidized low-density lipoproteins. *Am. J. Physiol. Gastrointest Liver Physiol.*, **300**, G71–G81.

24. Harris,E.N. and Weigel,P.H. (2008) The ligand-binding profile of HARE: hyaluronan and chondroitin sulfates A, C, and D bind to overlapping sites distinct from the sites for heparin, acetylated low-density lipoprotein, dermatan sulfate, and CS-E. *Glycobiology*, **18**, 638–648.

25. Schledzewski,K., Geraud,C., Arnold,B., Wang,S., Grone,H.J., Kempf,T., Wollert,K.C., Straub,B.K., Schirmacher,P., Demory,A. *et al.* (2011) Deficiency of liver sinusoidal scavenger receptors stabilin-1 and -2 in mice causes glomerulofibrotic nephropathy via impaired hepatic clearance of noxious blood factors. *J. Clin. Invest.*, **121**, 703–714.

26. Kzhyshkowska,J., Gratchev,A., Schmuttermaier,C., Brundiers,H., Krusell,L., Mamidi,S., Zhang,J., Workman,G., Sage,E.H., Anderle,C. *et al.* (2008) Alternatively activated macrophages regulate extracellular levels of the hormone placental lactogen via receptor-mediated uptake and transcytosis. *J. Immunol.*, **180**, 3028–3037.

27. Kzhyshkowska,J., Workman,G., Cardo-Vila,M., Arap,W., Pasqualini,R., Gratchev,A., Krusell,L., Goerdt,S. and Sage,E.H. (2006) Novel function of alternatively activated macrophages: stabilin-1-mediated clearance of SPARC. *J. Immunol.*, **176**, 5825–5832.

28. Zhou,B., Weigel,J.A., Fauss,L. and Weigel,P.H. (2000) Identification of the hyaluronan receptor for endocytosis (HARE). *J. Biol. Chem.*, **275**, 37733–37741.

29. Harris,E.N., Weigel,J.A. and Weigel,P.H. (2004) Endocytic function, glycosaminoglycan specificity, and antibody sensitivity of the recombinant human 190-kDa hyaluronan receptor for endocytosis (HARE). *J. Biol. Chem.*, **279**, 36201–36209.

30. McGary,C.T., Raja,R.H. and Weigel,P.H. (1989) Endocytosis of hyaluronic acid by rat liver endothelial cells. Evidence for receptor recycling. *Biochem. J.*, **257**, 875–884.

31. Kzhyshkowska,J., Gratchev,A. and Goerdt,S. (2006) Stabilin-1, a homeostatic scavenger receptor with multiple functions. *J. Cell. Mol. Med.*, **10**, 635–649.

32. Goerdt,S., Walsh,L.J., Murphy,G.F. and Pober,J.S. (1991) Identification of a novel high molecular weight protein preferentially expressed by sinusoidal endothelial cells in normal human tissues. *J. Cell Biol.*, **113**, 1425–1437.

33. Lonsdale,J., Thomas,J., Salvatore,M., Phillips,R., Lo,E., Shad,S., Hasz,R., Walters,G., Young,N., Siminoff,L. *et al.* (2015) *Webpage*. 4th edn. The Broad Institute of MIT and Harvard, GTExPortal, Boston.

34. Harris,E.N., Kyosseva,S.V., Weigel,J.A. and Weigel,P.H. (2007) Expression, processing, and glycosaminoglycan binding activity of the recombinant human 315-kDa hyaluronic acid receptor for endocytosis (HARE). *J. Biol. Chem.*, **282**, 2785–2797.

35. Gopalakrishnan,S. and Harris,E.N. (2011) In vivo liver endocytosis followed by purification of liver cells by liver perfusion. *J. Vis. Exp.*, **10**, 3138.

36. Seglen,P.O. (1976) Preparation of isolated rat liver cells. *Methods Cell Biol.*, **13**, 29–83.

37. von Kleist,L., Stahlschmidt,W., Bulut,H., Gromova,K., Puchkov,D., Robertson,M.J., MacGregor,K.A., Tomilin,N., Pechstein,A., Chau,N. *et al.* (2011) Role of the clathrin terminal domain in regulating coated pit dynamics revealed by small molecule inhibition. *Cell*, **146**, 471–484.

38. Pandey,M.S., Harris,E.N. and Weigel,P.H. (2015) HARE-mediated endocytosis of hyaluronan and heparin is targeted by different subsets of three endocytic motifs. *Int. J. Cell Biol.*, 524707.

39. Schindelin,J., Arganda-Carreras,I., Frise,E., Kaynig,V., Longair,M., Pietzsch,T., Preibisch,S., Rueden,C., Saalfeld,S., Schmid,B. *et al.* (2012) Fiji: an open-source platform for biological-image analysis. *Nat. Methods*, **9**, 676–682.

40. Teplova,M., Minasov,G., Tereshko,V., Inamati,G.B., Cook,P.D., Manoharan,M. and Egli,M. (1999) Crystal structure and improved

antisense properties of 2′-O-(2-methoxyethyl)-RNA. *Nat. Struct. Biol.*, **6**, 535–539.

41. Macia,E., Ehrlich,M., Massol,R., Boucrot,E., Brunner,C. and Kirchhausen,T. (2006) Dynasore, a cell-permeable inhibitor of dynamin. *Dev. Cell*, **10**, 839–850.
42. Hughes,J.A., Avrutskaya,A.V. and Juliano,R.L. (1994) Influence of base composition on membrane binding and cellular uptake of 10-mer phosphorothioate oligonucleotides in Chinese hamster ovary (CHRC5) cells. *Antisense Res. Dev.*, **4**, 211–215.
43. Beck,G.F., Irwin,W.J., Nicklin,P.L. and Akhtar,S. (1996) Interactions of phosphodiester and phosphorothioate oligonucleotides with intestinal epithelial Caco-2 cells. *Pharm. Res.*, **13**, 1028–1037.
44. Cirak,S., Arechavala-Gomeza,V., Guglieri,M., Feng,L., Torelli,S., Anthony,K., Abbs,S., Garralda,M.E., Bourke,J., Wells,D.J. *et al.* Exon skipping and dystrophin restoration in patients with Duchenne muscular dystrophy after systemic phosphorodiamidate morpholino oligomer treatment: an open-label, phase 2, dose-escalation study. *Lancet*, **378**, 595–605.
45. Lima,W.F., Prakash,T.P., Murray,H.M., Kinberger,G.A., Li,W., Chappell,A.E., Li,C.S., Murray,S.F., Gaus,H., Seth,P.P. *et al.* (2012) Single-stranded siRNAs activate RNAi in animals. *Cell*, **150**, 883–894.
46. Sehgal,A., Barros,S., Ivanciu,L., Cooley,B., Qin,J., Racie,T., Hettinger,J., Carioto,M., Jiang,Y., Brodsky,J. *et al.* (2015) An RNAi therapeutic targeting antithrombin to rebalance the coagulation system and promote hemostasis in hemophilia. *Nat. Med.*, **21**, 492–497.
47. Goldman,S.D., Funk,R.S., Rajewski,R.A. and Krise,J.P. (2009) Mechanisms of amine accumulation in, and egress from, lysosomes. *Bioanalysis*, **1**, 1445–1459.
48. Kzhyshkowska,J., Gratchev,A., Martens,J.H., Pervushina,O., Mamidi,S., Johansson,S., Schledzewski,K., Hansen,B., He,X., Tang,J. *et al.* (2004) Stabilin-1 localizes to endosomes and the trans-Golgi network in human macrophages and interacts with GGA adaptors. *J. Leukoc. Biol.*, **76**, 1151–1161.
49. Guo,F., Li,Y., Liu,Y., Wang,J., Li,Y. and Li,G. (2010) Inhibition of metastasis-associated lung adenocarcinoma transcript 1 in CaSki human cervical cancer cells suppresses cell proliferation and invasion. *Acta Biochim. Biophys. Sin. (Shanghai)*, **42**, 224–229.
50. Tani,H., Nakamura,Y., Ijiri,K. and Akimitsu,N. (2010) Stability of MALAT-1, a nuclear long non-coding RNA in mammalian cells, varies in various cancer cells. *Drug Discov. Ther.*, **4**, 235–239.
51. Hirose,Y., Saijou,E., Sugano,Y., Takeshita,F., Nishimura,S., Nonaka,H., Chen,Y.R., Sekine,K., Kido,T., Nakamura,T. *et al.* (2012) Inhibition of stabilin-2 elevates circulating hyaluronic acid levels and prevents tumor metastasis. *Proc. Natl. Acad. Sci. U.S.A.*, **109**, 4263–4268.
52. Stein,C.A. (2001) The experimental use of antisense oligonucleotides: a guide for the perplexed. *J. Clin. Invest.*, **108**, 641–644.
53. Doherty,G.J. and McMahon,H.T. (2009) Mechanisms of endocytosis. *Annu. Rev. Biochem.*, **78**, 857–902.
54. Zhou,B., Weigel,J.A., Saxena,A. and Weigel,P.H. (2002) Molecular cloning and functional expression of the rat 175-kDa hyaluronan receptor for endocytosis. *Mol. Biol. Cell*, **13**, 2853–2868.
55. Hansen,B., Longati,P., Elvevold,K., Nedredal,G.I., Schledzewski,K., Olsen,R., Falkowski,M., Kzhyshkowska,J., Carlsson,F., Johansson,S. *et al.* (2005) Stabilin-1 and stabilin-2 are both directed into the early endocytic pathway in hepatic sinusoidal endothelium via interactions with clathrin/AP-2, independent of ligand binding. *Exp. Cell Res.*, **303**, 160–173.
56. Prevo,R., Banerji,S., Ni,J. and Jackson,D.G. (2004) Rapid plasma membrane-endosomal trafficking of the lymph node sinus and high endothelial venule scavenger receptor/homing receptor stabilin-1 (FEEL-1/CLEVER-1). *J. Biol. Chem.*, **279**, 52580–52592.
57. Blundell,C.D., Almond,A., Mahoney,D.J., DeAngelis,P.L., Campbell,I.D. and Day,A.J. (2005) Towards a structure for a TSG-6.hyaluronan complex by modeling and NMR spectroscopy: insights into other members of the link module superfamily. *J. Biol. Chem.*, **280**, 18189–18201.
58. Seth,P.P. and Swayze,E.E. (2014) Unnatural Nucleoside Analogs for Antisense Therapy. In: Hanessian,S (ed). *Natural Products in Medicinal Chemistry*. Wiley-VCH Verlag GmbH & Co. KGaA, Weinheim, pp. 403–440.
59. Gilleron,J., Querbes,W., Zeigerer,A., Borodovsky,A., Marsico,G., Schubert,U., Manygoats,K., Seifert,S., Andree,C., Stoter,M. *et al.* (2013) Image-based analysis of lipid nanoparticle-mediated siRNA delivery, intracellular trafficking and endosomal escape. *Nat. Biotechnol.*, **31**, 638–646.
60. Del Buono,B.J., Luscinskas,F.W. and Simons,E.R. (1989) Preparation and characterization of plasma membrane vesicles from human polymorphonuclear leukocytes. *J. Cell. Physiol.*, **141**, 636–644.
61. Bermejo,M.K., Milenkovic,M., Salahpour,A. and Ramsey,A.J. (2014) Preparation of synaptic plasma membrane and postsynaptic density proteins using a discontinuous sucrose gradient. *J. Vis. Exp.*, e51896.